ACS Catalysis

Research Article

pubs.acs.org/acscatalysis

# Pd-Partially Reduced Graphene Oxide Catalysts (Pd/PRGO): Laser Synthesis of Pd Nanoparticles Supported on PRGO Nanosheets for Carbon–Carbon Cross Coupling Reactions

Sherif Moussa,[†] Ali R. Siamaki,[‡,†] B. Frank Gupton,[†,‡] and M. Samy El-Shall*[,†,‡]

[†]Department of Chemistry and [‡]Department of Chemical and Life Science Engineering, Virginia Commonwealth University, Richmond, Virginia 23284, United States

Supporting Information

**ABSTRACT:** This paper reports the development of a new family of highly active Pd nanoparticle catalysts supported on partially reduced graphene oxide nanosheets for carbon–carbon cross-coupling reactions. We report, for the first time, the synthesis of Pd nanoparticle catalysts supported on partially reduced graphene nanosheets (Pd/PRGO) by pulsed laser irradiation of aqueous solutions of graphene oxide and palladium ions without the use of chemical reducing or capping agents. The redox reactions initiated by the photoexcitation of GO using two 532 nm photons in different reducing environments of appropriate protic solvents (water, methanol, and ethanol) result in the formation of Pd nanoparticles with different sizes supported on the PRGO nanosheets. The laser irradiation process leads to the formation of multiple defect sites on the surface of the PRGO nanosheets which provide an excellent environment for anchoring the Pd nanoparticles, thus impeding the particles' migration and increasing the catalyst–support interaction. This consequently contributes to the enhanced catalytic performance and recyclability of the catalyst. The Pd/PRGO catalyst generated in water demonstrates excellent catalytic activity for Suzuki, Heck, and Sonogashira cross coupling reactions, with good recyclability for Suzuki coupling with a turn over number (TON) of 7800 and a remarkable turnover frequency (TOF) of 230,000 $h^{-1}$ at 120 °C under microwave heating. The results indicate that the defect sites generated on the PRGO nanosheets by the laser photochemical process play a major role in imparting the exceptional catalytic properties to these catalysts.

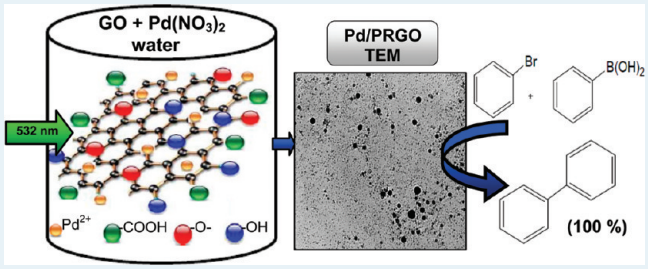


**KEYWORDS:** *graphene oxide, palladium catalyst, cross-coupling reactions, laser synthesis, graphene defects*

## INTRODUCTION

Graphene has been a subject of intense recent studies from both experimental and theoretical points of view because of its unique structural and electronic properties that include the highest intrinsic carrier mobility at room temperature of all known materials and very high mechanical strength and thermal stability.[1−6] These properties inspire many new applications in a wide range of areas including nanoelectronics, supercapacitors, batteries, photovoltaics, solar cells, fuel cells, transparent conducting films, sensors, and many others.[1−6] The recognition of this important new area of research and its tremendous potential applications have been highlighted by awarding the 2010 Nobel Prize in physics to Andre Geim and Konstantin Novoselov for "*groundbreaking experiments regarding the two-dimensional material graphene*".[7]

In addition to the unique electronic properties of graphene, other properties such as high thermal, chemical, and mechanical stability as well as high surface area also represent desirable characteristics as two-dimensional (2-D) support layers for metallic and bimetallic nanoparticles in heterogeneous catalysis.[12−25] The large surface area (2600 $m^2$ $g^{-1}$, theoretical value) of graphene and its high thermal and chemical stability provide an excellent catalyst support.[8−16] Supporting metal nanoparticles on graphene sheets could provide a large surface area and thermally stable system for potential applications in catalysis, fuel cells, chemical sensors, and hydrogen storage. In catalysis applications, unlike electronic applications, structural defects in the graphene lattice can be useful as they make it possible to tailor the localized properties of graphene to achieve new surface functionalities which could enhance the interactions with the anchored metal nanoparticles.[17,18]

One of the catalysis applications in which graphene support may provide some significant advantages is in the area of carbon–carbon cross coupling chemistry.[19−21] The development of palladium catalyzed cross-coupling reactions represents one of the most significant advancements in contemporary organic synthesis. This area of chemistry has increased the accessibility to molecules of greater chemical complexity, particularly in the area of pharmaceutical drug discovery and development.[22,23] In 2010 Richard Heck, Ei-ichi Negishi, and

Received: September 28, 2011
Revised: November 14, 2011
Published: December 1, 2011

  

Akira Suzuki received the Nobel Prize in Chemistry for their groundbreaking work in cross-coupling catalysis.[24] These reactions have typically been carried out under homogeneous reaction conditions, which require the use of ligands to stabilize the catalyst and broaden its window of reactivity.[24] However, the use of these catalysts under homogeneous conditions has limited their commercial viability because of product contamination as a direct result of an inability to effectively separate the catalyst from the reaction product.[22,25−28] The issue of product contamination is of particular importance in pharmaceutical applications where this chemistry is practiced extensively. Ligand-free heterogeneous palladium catalysis presents a promising option to address this problem as evidenced by the significant increase in research efforts in this area.[28−39]

Recently, we reported the remarkable cross-coupling catalytic activity of palladium nanoparticles deposited onto a graphene substrate.[15] The catalyst was prepared from palladium nitrate and graphene oxide using hydrazine hydrate as a reducing agent with microwave heating.[10,15] This procedure yielded highly uniform palladium nanoparticles which were evenly distributed across the graphene surface. These catalysts demonstrated extremely high turnover frequencies (108,000 $h^{-1}$) for Suzuki coupling reactions and were easily recovered and recycled under batch reaction conditions.[15] However, the major drawback of chemical reduction techniques is the difficulty in controlling the reduction process, as well as the use of toxic reducing agents which could be incorporated into the nanoparticles in the form of residual contamination. To overcome these problems, photochemical and photothermal reduction methods to prepare metal nanoparticles supported on graphene have been developed without a need for chemical reducing agents thus providing a green approach for the synthesis and processing of metal-graphene nanocomposites.[16,40−47] Other advantages of photochemical reactions include the possibility of creating structural defects on the graphene nanosheets which could lead to a stronger catalyst−support interaction by impeding particles' migration and thus contributing to an enhanced catalytic performance. One of the most efficient ways of controlling the types and density of defects on the graphene surface is by controlling the reduction of graphene oxide (GO) since GO is essentially a highly defective graphene sheet functionalized with oxygen atoms.[10,16,45−51] Through the control of the GO reduction process using different chemical and physical methods, the $sp^2$ domains of graphene can be partially restored, and the remaining structural defects can be used for the development of strong interaction sites with the metal nanoparticle catalysts.[10,16,46]

In this paper, we report the development of a facile laser reduction method for the synthesis of Pd nanoparticles supported on partially reduced graphene oxide (PRGO) and demonstrate their high activity for Suzuki, Heck, and Sonogashira cross-coupling reactions. The strategy adopted in developing this method utilizes the semiconductor properties of partially oxidized GO where domains of $sp^2$ and $sp^3$ carbon hybridization exist as the partial oxidation of graphite sheets takes place. Although fully oxidized GO is an insulator; partially oxidized GO has semiconductor properties with a bandgap that is determined by the extent of oxygenation of the graphite sheets which determines the size of the $sp^2$ $\pi$-conjugated domains.[47−52] The $sp^2$ domains act as semiconductors with bandgaps that increase with increasing the O/C ratio (2.5−4.0 eV depending on the O/C ratio).[52−57] Photoexcitation of the $sp^2$ domains in partially oxidized GO with light energy exceeding their bandgaps [for example, a single UV photon of 355 nm (3.5 eV) or two visible photons of 532 nm (2.3 eV)] results in the generation of an electron−hole pair within the semiconductor domain.[45−47] The photogenerated electrons in GO can lead to the reduction of the Pd ions simultaneously with the partial reduction of GO and thus the formation of Pd nanoparticles supported on the partially reduced graphene oxide (PRGO). The photogenerated holes can react with GO in the presence of water with evolution of CO and $CO_2$ gases thus creating structural defects within the PRGO nanosheets. By changing the solvent composition we are able to change the reducing environment and thus control the growth kinetics of the Pd nanoparticles and correlate the catalytic activity with the size of the Pd nanoparticles supported on the PRGO nanosheets. The results demonstrate the successful application of this method to prepare active Pd/PRGO nanocatalysts with tunable catalytic activities for cross-coupling reactions.

## EXPERIMENTAL SECTION

In the experiments, GO was prepared by the oxidation of high purity graphite powder (99.9999%, 200 mesh, Alfa Aesar) according to the method of Hummers and Offeman.[58] After repeated washing of the resulting yellowish-brown cake with hot water, the powder was dried at 60 °C in an oven overnight. For the laser synthesis of Pd/PRGO catalysts, 20 $\mu$L of $Pd(NO_3)_2$ was added to 6 mL of GO solution in 2 mg of GO/10 mL of deionized water (catalyst **A**). Similarly, 20 $\mu$L of $Pd(NO_3)_2$ was added to 6 mL of GO solution in 50 vol % ethanol−water (catalyst **B**) or 50% methanol−water mixtures (catalyst **C**). All solutions were stirred for 30 min prior to laser irradiation. The solutions were irradiated with a pulsed Nd:YAG laser (unfocused, second harmonic: $\lambda$ = 532 nm, 5 W, h$\nu$ = 2.32 eV, pulse width $\tau$ = 7 ns, repetition rate = 30 Hz, fluence ~0.1 J/$cm^2$, Spectra Physics LAB-170−30) under continuous stirring. The chemicals used were absolute methanol certified ACS with purity 99.9%, absolute ethanol anhydrous ACS/USP grade, and $Pd(NO_3)_2$ (10 wt % Pd in diluted $HNO_3$ acid, with purity 99.99%, Sigma-Aldrich).

The Pd/PRGO catalysts were separated and dried overnight under vacuum before the X-ray diffraction (XRD) or the X-ray photoelectron spectroscopy (XPS) measurements. Transmission electron microscopy (TEM) images were obtained using a Joel JEM-1230 electron microscope operated at 120 kV equipped with a Gatan UltraScan 4000SP 4k × 4k CCD camera. The XRD patterns were measured with an X'Pert Philips Materials Research Diffractometer using Cu $K_{\alpha 1}$ radiation. The XPS analysis was performed on Thermo Fisher Scientific ESCALAB 250 using a monochromatic Al KR. The Pd contents in the catalysts before and after the cross coupling reactions were determined using Inductive Coupled Plasma (ICP) Optical Emission Spectroscopy (Varian Vista-MPX CCD Simultaneous ICP-OES) and ICP Mass Spectrometry (ICP-MS, Varian 820-MS).

For the cross-coupling catalysis experiments, bromobenzene (50 mg, 0.32 mmol, 1 equiv) was dissolved in a mixture of 4 mL of $H_2O$:EtOH (1:1) and placed in a 10 mL microwave tube. To this mixture, phenyl boronic acid (47 mg, 0.38 mmol, 1.2 equiv) and potassium carbonate (133 mg, 0.96 mmol, 3 equiv) were added. The Pd/PRGO catalyst (**A** or **B** or **C**) (*X* mmol, *Y* mol % as indicated in Figure 4) was then added, and the tube was sealed and stirred at room temperature. An aliquot of the reaction mixture was taken after 30, 45, 60, 120, 180, 240, 300, 360, 420, 480


dx.doi.org/10.1021/cs200497e | ACS Catal. 2012, 2, 145−154

min and diluted with 10 mL of $CH_3CN$ and injected into the GC/MS instrument. The percent conversions of the products were then calculated based on the consumption of bromobenzene starting materials by means of GC-MS analysis. The characterization of the isolated products were carried out using $^1H$ NMR (300 MHz, $CDCl_3$), $^{13}C$ NMR (75.5 MHz, $CDCl_3$), and GC-MS (EI, 70 eV). Details of the catalysis experiments involving catalysts **A**, **B**, and **C**, and recycling experiments are given in Supporting Information.

## RESULTS AND DISCUSSION

**Laser Synthesis and Characterization of Pd/PRGO Nanocatalysts.** Figure 1-A displays the XRD patterns of GO

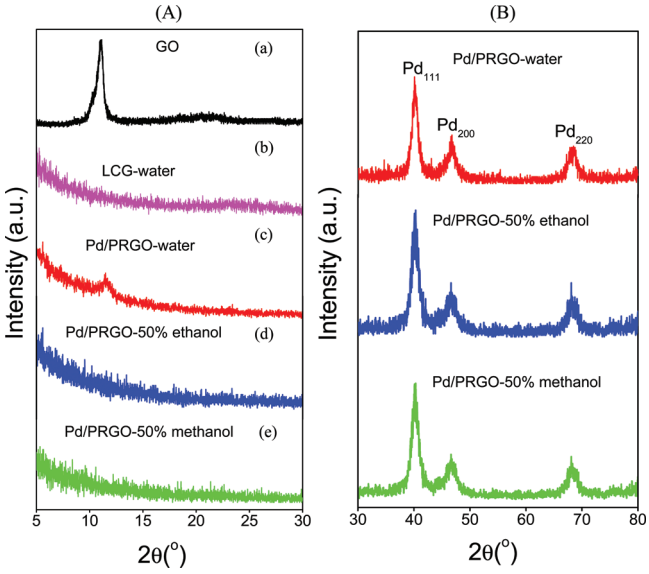


**Figure 1.** (A) XRD-patterns of GO before (a) and after (b) the 532 nm laser irradiation in water, and after laser irradiation in the presence of Pd ions in water (c), 50% ethanol–water (d), and 50% methanol–water (e) as solvents. (B) XRD patterns of the Pd-nanoparticles in the resulting Pd/PRGO after the 532 nm laser irradiation of $Pd(NO_3)_2$ in the presence of GO in water, 50% ethanol, and 50% methanol as solvents.

before (a) and after (b) the 532 nm laser irradiation in the absence of $Pd(NO_3)_2$ in water. The GO peak at $2\theta$ = 10.9° corresponds to a *d*-spacing of 8.14 Å resulting from the insertion of hydroxyl and epoxy groups between the graphite sheets as a result of the oxidation process of graphite.[10,45,46,48,59] Following the 532 nm laser irradiation for a few minutes, the yellow golden color of the GO solution in water changes to black with complete disappearance of the XRD 10.9° $2\theta$ peak suggesting the reduction of GO and the restoration of the $sp^2$ carbon sites in the laser converted graphene (LCG).[45,46] However, in the presence of $Pd^{2+}$ ions under identical conditions of GO concentration (0.2 mg/mL), solution volume (6 mL), and laser power (5 W, 30 Hz), a small appearance of the GO characteristic peak is still observed, as shown in Figure 1-A(c), suggesting a partial reduction of GO (PRGO). By using 50% ethanol–water and 50% methanol–water mixtures as solvents, a complete disappearance of the GO peak at $2\theta$ = 10.9° is observed after the laser irradiation in the presence of Pd ions under the same conditions mentioned above as shown in patterns (d) and (e) in Figure 1-A. The reduction of the Pd ions and the formation of Pd nanoparticles in the three solvents used are confirmed by the XRD patterns of the resulting Pd/PRGO catalysts as shown in Figure 1-B. The Pd-nanoparticles exhibit the typical face-centered-cubic (fcc) pattern of the Pd metal.[60] The irradiation time required for the formation of Pd/PRGO varies from a few to several minutes depending on the nature of the solvent, the laser power, the concentration of GO, and the volume of the solution. For example, under the conditions mentioned above, the formation of Pd/PRGO is completed after 3.5, 5, and 9 min in 50% methanol–water, 50% ethanol–water, and pure water, respectively. It should be noted that laser irradiation of the Pd nitrate precursors in water under identical solution concentration and laser irradiation conditions but in the absence of GO does not result in the formation of Pd nanoparticles. This indicates that the reduction of the Pd ions is directly coupled to the absorption of the 532 nm (two photons) light by GO, and thus laser excitation of GO must be involved in the reduction of Pd ions.

Figures 2-A, B, and C compare the C 1s XPS spectra of GO with that of the laser converted graphene (LCG) and the Pd/PRGO prepared in water, 50% ethanol–water, and 50% methanol–water, respectively. The GO spectrum shows peaks corresponding to oxygen containing groups between 285.5 and 289 eV, in addition to the $sp^2$-bonded carbon C=C at 284.5 eV. Typically, peaks at 285.6, 286.7, 287.7, and 289 are assigned to the C1s of the C–OH, C–O, C=O, and HO–C=O groups, respectively.[45,46,61,62] The XPS C 1s spectrum obtained following the 532 nm laser irradiation of GO in water in the absence of the Pd ions clearly indicates that most of the oxygen-containing groups in GO are removed consistent with the laser reduction of GO using the 532 nm photons as previously reported.[45,46] However, in the presence of the Pd ions, not all the oxygen-containing groups in GO are removed following the 532 nm laser irradiation as shown in the XPS data in Figure 2-A, suggesting that only partial reduction of GO occurs in the presence of Pd ions. Similar XPS results are obtained in the ethanol–water and methanol–water mixtures where only partial reduction of GO is observed in the presence of $Pd^{2+}$ ions as shown in Figures 2-B and 2-C, respectively. From the analysis of the C 1s XPS spectra shown in Figures 2-A, B, and C, the intensity ratio of the C=C to C–O peaks is found to increase from 0.67 in GO to 1.78 in Pd/PRGO-water, 3.40 in Pd/PRGO-50% ethanol, and 3.55 in Pd/PRGO-50% methanol. This indicates that the degree of the partial reduction of GO by the laser irradiation increases by increasing the reducing character of the solvent.[46] The partial reduction of GO in the presence of the $Pd^{2+}$ ions could be explained by a competition between the Pd ions and the $sp^2$ regions of GO for the photogenerated electrons in GO as observed in the photocatalytic reduction of $Au^{3+}$ and $Ag^+$ ions assisted by GO.[46]

Figure 2-D displays the XPS spectra of the Pd-3d electron in the Pd/PRGO catalysts prepared in water, 50% ethanol–water, and 50% methanol–water solvent systems. The data show that most of the Pd nanoparticles are present as Pd(0) consistent with the observed binding energies of 335 eV (Pd(0) $3d^{5/2}$) and 341.1 eV (Pd(0) $3d^{3/2}$).[63] As shown in Figure 2-D, the reference binding energies of the Pd(II)-3d electrons are significantly higher than the observed Pd(0) values.[63]

The Pd contents in the Pd-PRGO catalysts prepared in different solvent environments were determined using ICP-MS. Although the Pd contents in the initial solutions ($Pd(NO_3)_2$ + GO in water, 50% ethanol–water, or 50% methanol–water) were all similar (40 wt %), the amount of Pd deposited in each catalyst following the laser irradiation process was found to be


dx.doi.org/10.1021/cs200497e | ACS Catal. 2012, 2, 145–154

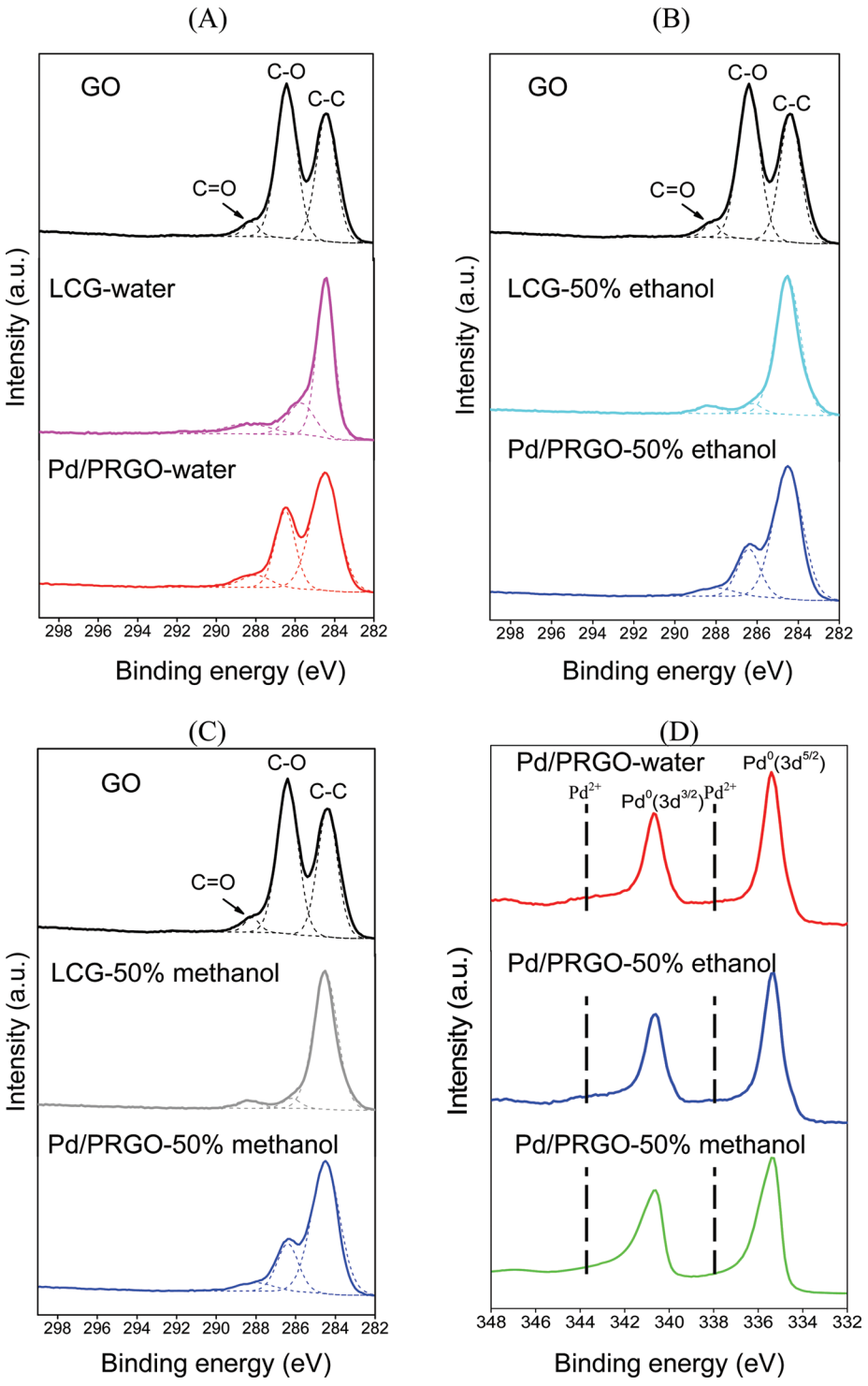


**Figure 2.** Comparisons of the XPS (C1s) binding energies of GO and that of the laser converted graphene (LGC) and Pd/PRGO prepared by the 532 nm laser irradiation (5 W, 30 Hz) of GO (0.2 mg/mL) or GO + Pd $(NO_3)_2$ in (A) water, (B) 50% ethanol–water, and (C) 50% methanol–water. (D) XPS (Pd-3d) binding energies of the Pd/PRGO catalysts prepared in different solvents as indicated. Dashed lines show the locations of the 3-d electron binding energies of $Pd^{2+}$.

different depending on the solvent environment. The Pd-PRGO catalyst prepared in pure water (catalyst **A**) has the lowest Pd content (18.2 wt %) followed by catalyst **B** prepared in 50% ethanol–water (24.3 wt %) and then catalyst **C** prepared in 50% methanol–water (29.4 wt %). The Pd content in the Pd/PRGO catalysts appears to increase with increasing the reducing environment of the solvent used. This also correlates with the laser irradiation times [under similar conditions: 20 $\mu$L $Pd(NO_3)_2$ in 6 mL of GO solution (2 mg GO/10 mL water), 532 nm laser, 5 W, 30 Hz] required for the reduction of the Pd ions and the partial reduction of GO (9, 5, and 3.5 min in pure water, 50% ethanol–water and 50% methanol–water, respectively).

Figure 3 displays representative TEM images of the Pd/PRGO catalysts (**A**, **B**, and **C**) prepared in pure water, 50% ethanol–water and 50% methanol–water, respectively as


dx.doi.org/10.1021/cs200497e | *ACS Catal.* 2012, 2, 145–154

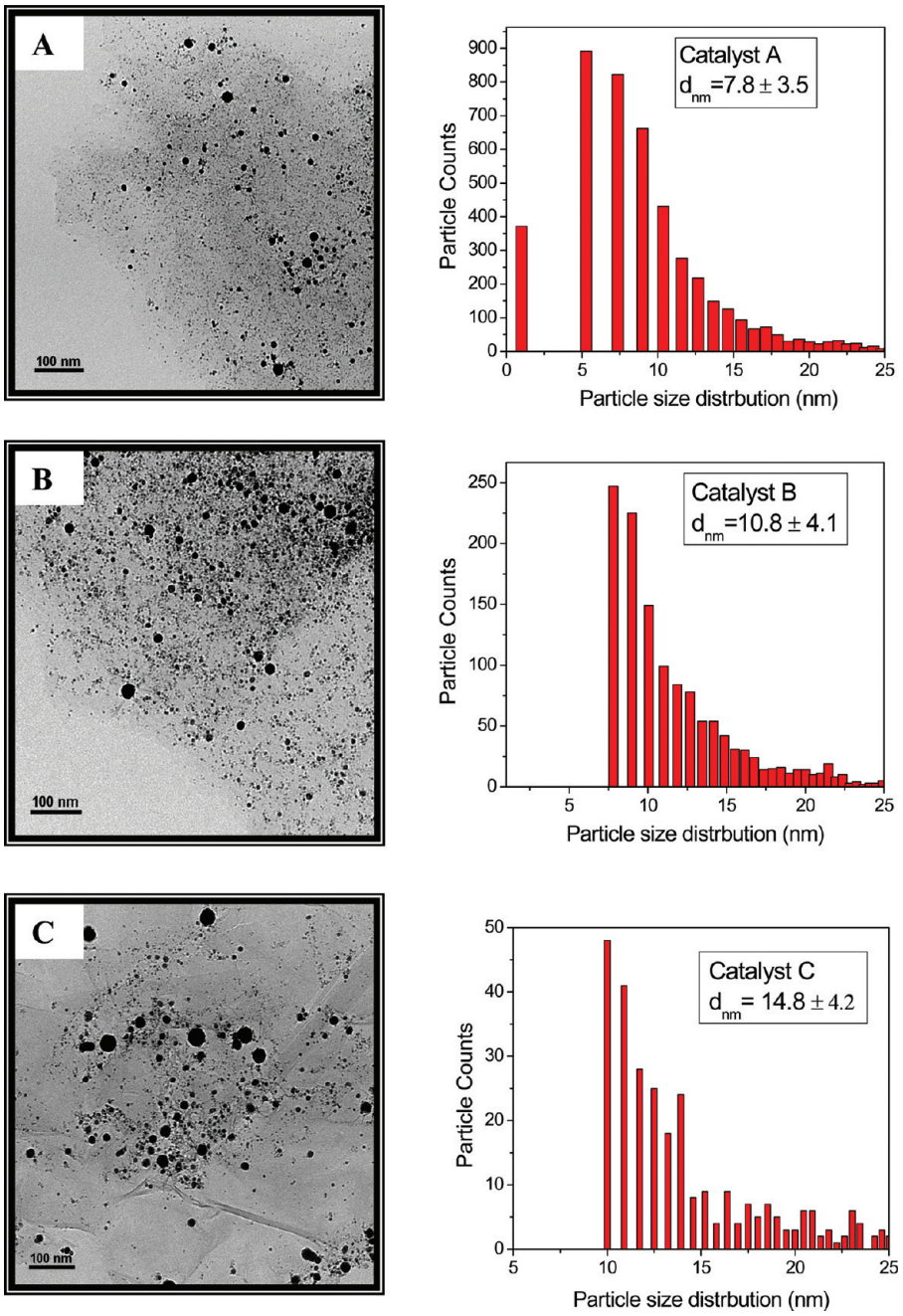


**Figure 3.** TEM images and particle size distributions of the Pd/PRGO catalysts **A**, **B**, and **C** prepared in pure water, 50% ethanol–water, and 50% methanol–water, respectively.

described above. From the measured particle size distributions shown in Figure 3, it is clear that catalyst **A** prepared in pure water has the smallest Pd-nanoparticles with an average size of 7.8 ± 3.5 nm followed by catalyst **B** (prepared in 50% ethanol–water mixture) with an average Pd particle size of 10.8 ± 4.1 nm, and then catalyst **C** (prepared in 50% methanol–water mixture) where the average particle size is 14.8 ± 4.2 nm. It is interesting to note that catalyst **A** contains a significant number of very small Pd nanoparticles in the size range of 1–2 nm as shown in the TEM image of catalyst **A**. These very small particles were not accurately accounted for in the calculations of the average particle sizes shown in Figure 3, and therefore, the reported averages are considered upper limits of the actual particle size ranges. The TEM results are consistent with both the ICP-MS data and the laser irradiation times which together confirm the general trend that increasing the reducing environment of the solvent during the laser irradiation of the GO-$Pd(NO_3)_2$ mixture results in a rapid reduction of the Pd ions and an increase in the growth rate of the resulting Pd nanoparticles, and consequently an increase in the average size and the degree of agglomeration of the final Pd nanoparticles supported on the PRGO nanosheets.

**Mechanism of Partial Reduction of GO and Defect Generation.** The above results not only provide direct evidence for the formation of Pd nanoparticles on partially reduced GO following the 532 nm laser irradiation of the GO-$Pd(NO_3)_2$ mixture in different solvent environments, but they also shed light on the reduction mechanism of the $Pd^{2+}$ ions


dx.doi.org/10.1021/cs200497e | *ACS Catal.* 2012, 2, 145–154

and the partial reduction of GO. As indicated earlier, partially oxidized GO contains a mixture of hydrophobic $\pi$-conjugated $sp^2$ and hydrophilic oxygen-containing $sp^3$ domains which lead to semiconductor properties with a bandgap that depends on the extent of oxygenation of graphite (2.5–4.0 eV depending on the O/C ratio).[52−57,64,65] Absorption of two 532 nm photons generates an electron–hole pair ($e^-$-$h^+$) within the semiconductor GO (Reaction 1).[45−47] The photogenerated electrons in GO are used for the reduction of the $Pd^{2+}$ ions (Reaction 2) simultaneously with partial reduction of GO depending on the solvent environment.[47] In the presence of a reducing environment provided by ethanol (Scheme 1), the holes are scavenged to produce protons and reducing ethoxy radicals. Since the ethoxy radicals ($^{\bullet}C_2H_4OH$) are strong reducing agents they undergo oxidation to $CH_3CHO$ and therefore reduce GO.[43,44,66] This is consistent with increasing the degree of reduction of GO in the presence of alcohols.

$$GO + h\nu \rightarrow GO(h^+ + e^-) \quad (1)$$

$$M^+ + GO(e^-) \rightarrow GO + M \quad (2)$$

**Scheme 1**

$$h^+ + C_2H_5OH \rightarrow {}^{\cdot}C_2H_4OH + H^+ \quad (3)$$

$$M^+ + GO(e^-) \rightarrow GO + M \quad (4)$$

$$n\,{}^{\cdot}C_2H_4OH + GO \rightarrow RGO + n\,CH_3CHO + n/2\,H_2O \quad (5)$$

In the presence of methanol, $CO_2$ and $H_2$ gases can be produced according to Scheme 2.[66] (Reactions 6, 7)

**Scheme 2**

$$6h^+ + CH_3OH + 6OH^- \rightarrow CO_2 + 5\,H_2O \quad (6)$$

$$6H^+ + 6e^- \rightarrow 3H_2 \quad (7)$$

In the absence of a reducing environment as in pure water, the photogenerated holes can react with the oxygen containing functional groups of GO and water to produce $CO_2$ and protons and result in the formation of carbon defect sites in GO (Reactions 8, 10).[47] The electrons and protons remove OH or oxygen groups from the GO to form $H_2O$ (Reactions 9, 11). These reactions result in the significant number of carbon defect sites in GO which are considered important active sites for the production of $H_2$.[47] Scheme 3 describes the formation

**Scheme 3**

For the hydroxyl group in GO

$$C\text{-}C\text{-}OH\ (GO) + H_2O + 3h^+ \rightarrow C\ (\text{defect carbon}) + CO_2 + 3H^+ \quad (8)$$

$$C\text{-}C\text{-}O\text{-}H\ (GO) + H^+ + e^- \rightarrow C\text{-}C\ (\text{defect carbon}) + H_2O \quad (9)$$

For the epoxy group in GO

$$C\text{-}O\text{-}C\ (GO) + H_2O + 2h^+ \rightarrow C\ (\text{defect carbon}) + CO_2 + 2H^+ \quad (10)$$

$$C\text{-}O\text{-}C\ (GO) + 2H^+ + 2e^- \rightarrow C\text{-}C\ (\text{defect carbon}) + H_2O \quad (11)$$

of carbon defect sites through the photoreaction of water with the hydroxyl and epoxy groups of GO.[47]

**Application of Pd/PRGO Nanocatalysts for Suzuki Reaction.** In this section we investigate the catalytic activity of the Pd-PRGO nanocatalysts **A**, **B**, and **C** produced by the 532 nm laser irradiation of $Pd(NO_3)_2$–GO mixtures in water, 50% ethanol, and 50% methanol as solvents, respectively for cross coupling reactions. Figure 4 illustrates the catalytic activity of the three catalysts at different catalyst loadings using Suzuki cross coupling reaction of bromobenzene and phenyl boronic acid in a mixture of $H_2O$:EtOH (1:1) at room temperature (Reaction 12).

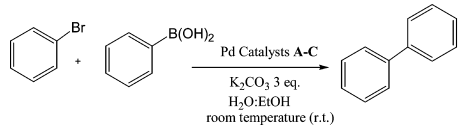


(12)

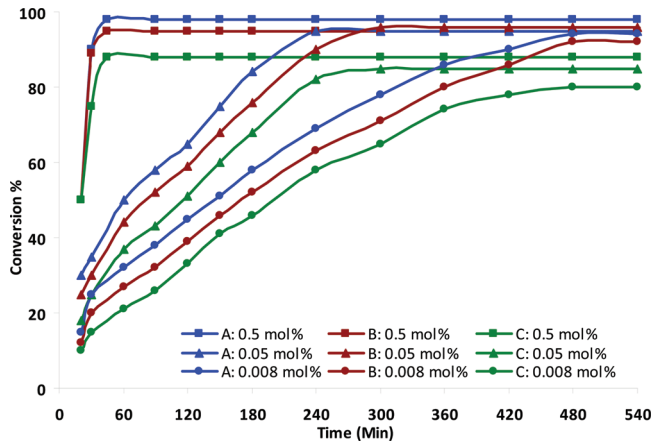


**Figure 4.** Effect of concentration of the Pd/PRGO catalysts **A**, **B**, and **C** on the conversion of Suzuki reaction (Reaction 12).

As shown in Figure 4, at 0.5 mol % concentration, catalysts **A** and **B** show similar reactivity and result in a high conversion of 100% and 95%, respectively after 45 min reaction time at room temperature. Catalyst **C** shows only 88% conversion within 45 min under these conditions. Similarly, at lower catalyst loading of 0.05 mol %, catalysts **A** and **B** work effectively, giving a conversion of 95% and 90%, respectively after 4 h at room temperature. Catalyst **C** gives only 82% yield under these conditions. A similar trend is observed when the amount of catalyst loading is decreased to 0.008 mol % in which catalysts **A**, **B**, and **C** result in 95, 92, and 80% conversions, respectively, after 8 h at room temperature. Interestingly, when the same Pd loading of 0.008 mol % is applied at 120 °C under microwave irradiation (MWI), the reaction is surprisingly fast for catalyst **A**, converting 62% of bromobenzene after 2 min. Continuing the reaction under the same conditions (120 °C, MWI) leads to complete formation of the biphenyl (100%) product after 5 min. It should be noted that at this very low catalyst loading (0.008 mol %), higher microwave heating of 120 °C was required to afford a full conversion to the Suzuki product. The 100% conversion of the 0.008 mol % catalyst **A** indicates a remarkable turn over number (TON) of 7800 and a turnover frequency (TOF) of 230,000 $h^{-1}$ for a microwave assisted Suzuki cross coupling reaction at 120 °C. However, with 0.008 mol % of catalyst **B**, the Suzuki reaction of bromobenzene and phenyl boronic acid results in a 45% formation of the biphenyl product after 2 min at 120 °C under MWI. This reaction is also completed after 5 min under MWI at 120 °C. This provides a TON of 5600 and a TOF of 169,000 $h^{-1}$ for the Pd/PRGO catalyst **B** for a microwave assisted Suzuki cross coupling reaction at 120 °C.


dx.doi.org/10.1021/cs200497e | ACS Catal. 2012, 2, 145–154

The possibility of formation of the biphenyl product by a homocoupling process was investigated by carrying out the reaction of 4-bromoanisole with phenyl boronic acid in the presence of 0.5 mol % of the Pd/PRGO catalyst **A** and potassium carbonate at 80 °C microwave irradiation for 5 min. Analysis of the reaction mixture by GC-MS revealed the formation of 4-methoxy-1,1′-Biphenyl ($m/z$ = 184), as the only product of this reaction in 100% conversion. No evidence for any homocoupled products such as biphenyl or 1,1′-biphenyl-4,4-dimethoxy was observed. This result confirms the formation of the biphenyl products by the Suzuki cross coupling reaction.

It is interesting to note that when a similar Suzuki cross coupling reaction (bromobenzene and phenyl boronic acid with potassium carbonate in a mixture of $H_2O$:EtOH (1:1) at 120 °C) was performed under conventional thermal heating using 0.008 mol % of catalyst **A**, only a small conversion of 5% was observed after 6 h refluxing conditions at 120 °C. This result clearly demonstrates the effect of microwave irradiation in increasing reaction rates by providing a direct and rapid heating source for the cross coupling reactions.[15] This observation is consistent with recent reports on the selective heating of the surface of the heterogeneous catalysts and the formation of hot-spots by microwave irradiation which can lead to non-equilibrium local heating at the surface of the metal nanoparticle catalysts.[67−69]

The activity and recyclability of catayst **A** are truly remarkable considering that the ICP-MS analysis indicates that this catalyst (prepared in pure water) has the lowest Pd content (18.2 wt %) as compared to catalyst **B** (prepared in 50% ethanol−water, 24.3 wt % Pd) and catalyst **C** (prepared in 50% methanol−water, 29.4 wt % Pd). However, the high activity of catalyst **A** correlates nicely with the smallest average size of the Pd nanoparticles (7.8 ± 3.5 nm) as compared to catalyst **B** (10.8 ± 4.1 nm) and catalyst **C** (14.8 ± 4.2 nm) as shown in Figure 3. Catalyst **A** also exhibits well-dispersed Pd nanoparticles on the PRGO nanosheets with no evidence of significant particle agglomeration as shown in the TEM images of Figure 3. As discussed above, increasing the reducing environment of the solvent during the laser irradiation of the GO-$Pd(NO_3)_2$ mixture results in a rapid reduction of the Pd ions and an increase in the growth rate of the resulting Pd nanoparticles, and consequently an increase in the average size and the degree of agglomeration of the final Pd nanoparticles supported on the PRGO nanosheets as clearly demonstrated in catalyst **C**. We also believe that the reduction mechanism discussed above plays an important role in the remarkable activity and reusability of catalyst **A**. Specifically, the reduction of the oxygen containing functional groups of GO into carbon defect sites as a result of the reactions of water with the photoexcited GO appears to play a major role in imparting the exceptional catalytic properties to catalyst **A**. These defect sites can provide favorable structural environment and possible electronic interaction for anchoring the palladium nanoparticles on the surface of the PRGO nanosheets.

**Recyclability of the Pd/PRGO Nanocatalysts in Suzuki Reaction.** A significant practical application of heterogeneous catalysis is in the ability to easily remove the catalyst from the reaction mixture and reuse it for subsequent reactions until the catalyst is sufficiently deactivated. The recyclability of the Pd/PRGO nanocatalysts **A** and **B** was examined using the Suzuki cross coupling reaction of bromobenzene and phenyl boronic acid at 80 °C under microwave heating utilizing 0.5 mol % of catalyst loading. After each run, catalyst was removed by simple washing with ethanol followed by decantation and reused for subsequent reaction. The results from the recycling experiments are shown in the Supporting Information, Table S1. For catalyst **A**, the completion of reaction was accomplished after 5 min for the first four runs. The catalytic activity dropped to 60% in the fifth and 6th runs, 50% in run seven, and then significantly dropped below 50% for the next recycling reactions. For catalyst **B**, full conversions were obtained in the first two runs. The activity slightly dropped in the third run, yielding 86% conversion. The catalytic activity was further decreased in runs 4 and 5 to 63% and 50% conversions, respectively. Lower conversions of below 50% were achieved after the fifth run. In contrast to catalysts **A** and **B**, no effective recyclability was found for catalyst **C**. This catalyst gave a 100% conversion only for the first run, and activity was then diminished to 65 and 54% and even lower for the subsequent runs.

It is instructive to compare the performance of the current Pd/PRGO catalysts with other Pd nanoparticle catalysts developed for cross coupling reactions. There are many examples in the literature of Pd nanoparticles stabilized by capped polymeric materials for cross coupling reactions, and in particular Suzuki reactions.[28−39] These include Pd nanoparticles stabilized by polyvinyl pyrrolidone (PVP), and some few examples on using polystyrene-polyethylene oxide (PS-PEO), and poly(amido-amine) dendrimers (PAMAM) as well as other polymers.[39] Although these nanocatalysts demonstrated reactivity toward Suzuki reactions, most catalysts have shown some limited catalytic activity such as lower product yields using low catalyst loadings, lack of efficient recyclability and low TON and TOF.[39] For example, the yields of the biphenyl products using the Pd-PVP and Pd-MAMAM nanoparticles were found to be 39% and 34%, respectively for the first cycle of the reaction and significantly lowers yields for the second cycle.[31] In addition, it has been found that in case of Pd supported on PVP, increasing the amount of the PVP stabilizer resulted in decreasing the catalyst activity in the Suzuki reactions because of the capping effect of the PVP which reduces the access to the active coordination sites on the metal center for the catalysis.[30] Another example also includes the Pd-PVP catalysts with very low catalyst loadings (ca. 0.005−0.01 mol %) under microwave reaction conditions which resulted in 75−79% and 43−87% yields for aryl iodides and bromides, respectively.[35] However, Pd nanoparticles stabilized by poly(*N*,*N*-dihexylcarbodiimide) were found to be active in the coupling reactions of aryl iodides and bromides using higher catalyst loadings (0.5 mol %) under microwave conditions, and they could be recycled up to five times with slightly decreased activity.[36] Recently, microporous polymers have been used as both stabilizer and support for the Pd nanoparticles and resulted in highly recyclable catalysts for the Suzuki coupling of bromoacetophenone and phenylboronic acid (up to 9 times using 0.3 mol % catalyst loading).[37] On the basis of these and other examples discussed in ref 39, it can be concluded that the current Pd/PRGO nanoparticles provide highly stable and efficient catalysts for cross coupling reactions as compared to other Pd nanoparticles stabilized by polymeric molecules.[39]

To understand the deactivation mechanism of the Pd/PRGO catalysts, TEM images of catalysts **A** and **B** were obtained after the first run and also after the seventh for catalyst A and after the 6th run for catalyst B as shown in Figure 5. It is clear that the degree of agglomeration of catalyst **A** does not change


dx.doi.org/10.1021/cs200497e | *ACS Catal.* 2012, 2, 145−154

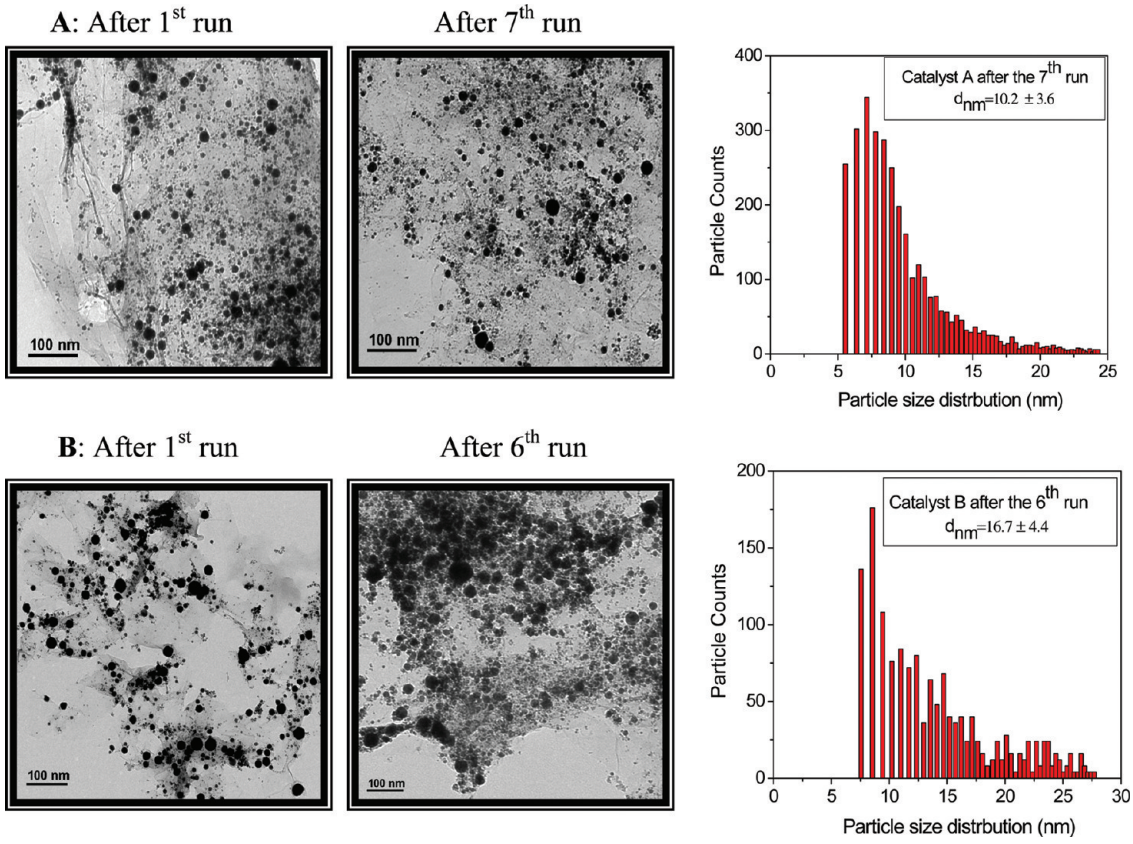


**Figure 5.** (Top) TEM images of catalyst **A** after the 1st and 7th runs and the particle size distribution after the 7th run. (Bottom) TEM images of catalyst **B** after the 1st and 6th runs and the particle size distribution after the 6th run.

much between the first and the seventh runs consistent with the ability to efficiently recycle this catalyst four times without loss of activity. It is also clear that catalyst **B** shows more significant agglomeration of the Pd nanoparticles after the 6th run than catalyst **A** after the seventh run. This is consistent with higher activity and better recyclability of catalyst **A** as compared to catalyst **B**. This result indicates that the mechanism of deactivation is likely to involve the formation of agglomerated Pd nanoparticles which leads to the decrease of the surface area and saturation of the coordination sites. This is consistent with the lower activity and lack of recyclability of catalyst **C**. As shown in Figure 3, catalyst **C** has the largest average particle size distribution of the Pd nanoparticles (14.8 ± 4.2 nm), and the TEM image shown in Figure 3-C indicates a significant agglomeration of the Pd nanoparticles on the PRGO nanosheets. As explained above, the rapid reduction conditions of the $Pd^{2+}$ ions in the presences of methanol (catalyst **C**) leads to rapid growth of the Pd nanoparticles which results in larger particle sizes and significant agglomeration.

To further evaluate the nature of the catalytic mechanism of the Pd/PRGO catalysts, we performed the Suzuki reaction of bromobenzene and phenyl boronic acid in the presence of 0.5 mol % of the Pd/PRGO catalyst (**A**, **B**, or **C**) and potassium carbonate at 80 °C microwave irradiation for 5 min. The reaction mixtures were hot filtered over celite after the first run, and the filtrate solutions were subjected to ICP-OES where the Pd contents were measured as 350, 780, and 1150 ppb in the solutions of catalysts **A**, **B**, and **C**, respectively. It should be noted that celite is a naturally occurring earth mineral with particle sizes ranging from 1 $\mu$m to 1 mm with high porosity, and therefore, it is not capable of removing any homogeneous particles and species from the reaction mixture. Furthermore, the Pd contents of catalysts **A** and **B** determined in solutions by ICP-MS after the 7th and 6th runs, respectively, were found to be 458 and 738 ppb for catalyst **A** and **B**, respectively. It is interesting, however, to note that the Pd content in the reaction solution of catalyst **A** after the seventh run is significantly smaller as compared to the solution of catalyst **B** after the 6th run. This could suggest stronger interaction of the Pd nanoparticles with the PRGO nanosheets in catalyst **A** than in catalyst **B**, consistent with the presence of a significant number of carbon defect sites in catalyst **A** as discussed above. These defects could impede particle migration and increase the catalyst–support interaction and consequently contribute to the enhanced catalytic performance of catalyst **A**.

It should be noted that simple physical mixing of preformed small Pd nanoparticles (4–6 nm) and reduced GO sheets results in significant aggregation of the Pd nanoparticles with a very poor dispersion on the graphene sheets as has been reported recently.[10] However, the simultaneous photoreduction of the Pd ions and the partial reduction of GO demonstrated here appears to provide strong interaction between the Pd nanoparticles and the PRGO nanosheets through the defect sites in the PRGO. This strong catalyst–support interaction is essential for the dispersion of the Pd nanoparticles and consequently the high catalytic activity and recyclability of the Pd/PRGO catalysts.

We note that the small amounts of leached palladium from the Pd/PRGO catalysts may not be consistent with a complete heterogeneous catalytic system.[39] However, further evidence on the nature of the catalytic mechanism is the failure to observe reactivity after the removal of the supported nanoparticles from


dx.doi.org/10.1021/cs200497e | *ACS Catal.* 2012, 2, 145–154

the reaction medium by filtration over celite. Thus, the present results provide direct implication for the dominant release and redeposition catalytic mechanism, by which a small quantity of Pd leaches into the reaction solution, catalyzes the reaction, and redeposits to the surface of the graphene support at the end of the reaction. In this case, either "naked Pd atoms" could be released to the solution from the Pd nanoparticles supported on the PRGO nanosheets or oxidative addition of bromobenzene on the Pd nanoparticles' surface occurs where the oxidized Pd species are detached from the surface to the solution.[39,70,71] This mechanism is consistent with Pd nanoparticles acting as a reservoir of molecular species where the leaching can be reversible and Pd nanoparticles can be formed in solution and redeposited on the PRGO surface. In this case, the large surface area created by the PRGO support can effectively facilitate both the dispersion of the Pd nanoparticles as a heterogeneous catalyst system and also the possible Pd leaching into the solution to catalyze the reaction followed by deposition of the leached Pd on the surface of the support after the reaction is completed.

**Applications of the Pd/PRGO Catalyst A for Heck and Sonogashira Reactions.** The utility of laser synthesized Pd/PRGO catalyst **A** was further evaluated for other carbon−carbon bond forming processes such as the Heck and Sonogashira reactions.[72,73] While these reactions are typically carried out in the presence of a homogeneous palladium catalyst and appropriate ligands,[19−22,72,73] we were set to examine the Pd/PRGO catalysts under ligandless microwave irradiation conditions.[15] Thus, the reactions of iodobenzene with styrene or phenyl acetylene, and potassium carbonate in $H_2O$:EtOH solvents were investigated in the presence of 0.5 mol % catalyst **A**, under microwave heating at 180 °C for 10 min. As shown in Scheme 4, both these reactions can be successfully performed

**Scheme 4. Heck and Sonogashira Coupling Reaction Using the Pd/PRGO Catalyst A**

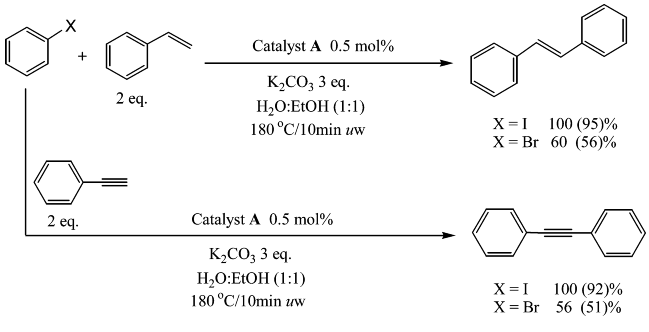


under these conditions, providing a complete conversions of 100% and high isolated yields of 95 and 92% of the corresponding Heck and Sonogashira products, respectively. Utilizing bromobenzene as the starting materials afforded lower conversions of 60 and 56% for the Heck and Sonogashira reactions, respectively. With a more difficult substrate such as 4-nitro-1-chlorobenzene, however, there were only 10−15% conversions for both Heck and Sonogashira reactions.

## CONCLUSIONS

The results presented here demonstrate, for the first time, the synthesis of Pd nanoparticle catalysts supported on partially reduced graphene nanosheets (Pd/PRGO) by the pulsed laser irradiation of solutions of graphene oxide and palladium ions. The reported method does not require the use of chemical reducing or capping agents to control the growth kinetics of the Pd nanoparticle catalysts. The method can lead to controlling the particle size distribution and the degree of dispersion of the Pd nanoparticles, and to the generation of carbon defect sites for anchoring the Pd nanoparticle catalysts on the PRGO nanosheets. The Pd/PRGO catalyst prepared by the laser induced photochemical reaction of graphene oxide with water in the presence of palladium ions exhibit exceptional catalytic activity and good recyclability for Suzuki cross coupling reaction with a remarkable TON of 7800 and a TOF of 230,000 $h^{-1}$ at 120 °C under microwave heating. The defect sites generated on the PRGO nanosheets by the photochemical process appear to play a major role in imparting the exceptional catalytic properties to the catalyst.

## ASSOCIATED CONTENT

### Supporting Information

Details of the catalysis reactions and catalyst recycling experiments and a table of the catalyst recycling results. This material is available free of charge via the Internet at http://pubs.acs.org.

## AUTHOR INFORMATION

### Corresponding Author

*E-mail: mselshal@vcu.edu.

### Funding

We thank the National Science Foundation (CHE-0911146) for the support of this work.

## REFERENCES

(1) Geim, A. K. *Science* **2009**, *324*, 1530−1534.
(2) Novoselov, K. S.; Geim, A. K.; Morozov, S. V.; Jiang, D.; Katsnelson, M. L.; Grigorieva, I. V.; Dubonos, S. V.; Firsov, A. A. *Nature* **2005**, *438*, 197−200.
(3) Novoselov, K. S.; Jiang, Z.; Zhang, Y.; Morozov, S. V.; Stormer, H. L.; Zeitler, U.; Maan, J. C.; Boebinger, G. S.; Kim, P.; Geim, A. K. *Science* **2007**, *315*, 1379.
(4) Allen, M. J.; Tung, V. C.; Kaner, R. B. *Chem. Rev.* **2009**, *110*, 132−145.
(5) Rao, C. N. R.; Sood, A. K.; Subrahmanyam, K. S.; Govindaraj, A. *Angew. Chem., Int. Ed.* **2009**, *48*, 7752−7777.
(6) Wu, J.; Pisula, W.; Mullen, K. *Chem. Rev.* **2007**, *107*, 718−747.
(7) The Nobel Prize in Physics 2010 was awarded jointly to Andre Geim and Konstantin Novoselov *"for groundbreaking experiments regarding the two-dimensional material graphene"*, http://nobelprize.org/nobel_prizes/physics/laureates/2010/press.html.
(8) Kamat, P. V. *J. Phys. Chem. Lett.* **2010**, *1*, 520−527.
(9) Si, Y. C.; Samulski, E. T. *Chem. Mater.* **2008**, *20*, 6792−6797.
(10) Hassan, H. M. A.; Abdelsayed, V.; Khder, A. E. R.; AbouZeid, K. M.; Terner, J.; El-Shall, M. S.; Al-Resayes, S. I.; El-Azhary, A. A. *J. Mater. Chem.* **2009**, *19*, 3832−3837.
(11) Goncalves, G.; Marques, P. A. A. P.; Granadeiro, C. M.; Nogueira, H. I. S.; Singh, M. K.; Gracio, J. *Chem. Mater.* **2009**, *21*, 4796−4802.
(12) Scheuermann, G. M.; Rumi, L.; Steurer, P.; Bannwarth, W.; Mülhaupt, R. *J. Am. Chem. Soc.* **2009**, *131*, 8262.
(13) Jin, Z.; Nackashi, D.; Lu, W.; Kittrell, C.; Tour, J. M. *Chem. Mater.* **2010**, *22*, 5695−5699.
(14) Jasuja, K.; Linn, J.; Melton, S.; Berry, V. *J. Phys. Chem. Lett.* **2010**, *1*, 1853−1860.
(15) Siamaki, A. R.; Khder, A. E. R. S.; Abdelsayed, V.; El-Shall, M. S.; Gupton, B. F. *J. Catal.* **2011**, *279*, 1−11.

(16) Moussa, S.; Abdelsayed, V.; El-Shall, M. S. *Chem. Phys. Lett.* **2011**, *510*, 179−184.
(17) Banhart, F.; Kotakoski, J.; Krashennnikov, A. V. *ACS Nano* **2011**, *5*, 26−41.
(18) Kim, G.; Jhi, S.-H. *ACS Nano* **2011**, *5*, 805.
(19) Special Issue on "Cross Coupling": Buchwald, S. L., Ed.; *Acc. Chem. Res.* **2008**, *41*, 1439−1564.
(20) *Handbook of Organopalladium Chemistry for Organic Synthesis*; Negishi, E., de Mrijere, A., Eds.; Wiley-Interscience: New York, 2002.
(21) Yin, L.; Liebscher, J. *Chem. Rev.* **2007**, *107*, 133.
(22) de Vries, J. G. *Can. J. Chem.* **2001**, *79*, 1086.
(23) Zapf, A.; Beller, M. *Top. Catal.* **2002**, *19*, 101.
(24) The Nobel Prize in Chemistry 2010 was awarded jointly to Richard F. Heck, Ei-ichi Negishi, and Akira Suzuki *"for palladium-catalyzed cross couplings in organic synthesis"*. http://nobelprize.org/nobel_prizes/chemistry/laureates/2010/press.html
(25) Garrett, C.; Prasad, K. *Adv. Synth. Catal.* **2004**, *346*, 889.
(26) Cole-Hamilton, D. J. *Science* **2003**, *299*, 1702.
(27) Widegren, J. A. *J. Mol. Catal. A* **2003**, *198*, 317.
(28) Welch, C. J.; Albaneze-Walker, J.; Leonard, W. R.; Biba, M.; DaSilva, J.; Henderson, D.; Laing, B. B.; Mathre, D. J.; Spencer, S.; Bu, X.; Wang, T. *Org. Process Res. Dev.* **2005**, *9*, 198.
(29) Köhler, K.; Heidenreich, R. G.; Soomro, S. S.; Pröckl, S .S. *Adv. Synth. Catal.* **2008**, *350*, 2930.
(30) Narayanan, R.; El-Sayed, M. A. *J. Am. Chem. Soc.* **2003**, *125*, 8340.
(31) Narayanan, R.; El-Sayed, M. A. *J. Phys. Chem. B* **2004**, *108*, 8572.
(32) Duanmu, C.; Saha, I.; Zheng, Y.; Goodson, B. M.; Gao, Y. *Chem. Mater.* **2006**, *18*, 5973.
(33) Narayanan, R.; Tabor, M.; El-Sayed, M. *Top. Catal.* **2008**, *48*, 60.
(34) Ellis, P. J.; Fairlamb, I. J. S.; Hackett, S. F. J.; Wilson, K.; Lee, A. F. *Angew. Chem., Int. Ed.* **2010**, *49*, 1820.
(35) Martins, D. L.; Alvarez, H. M.; Aguiar, L. C. S. *Tetrahedron Lett.* **2010**, *51*, 6814.
(36) Liu, Y.; Khemtong, C.; Hu, J. *Chem. Commun.* **2004**, 398.
(37) Ogasawara, S.; Kato, S. *J. Am. Chem. Soc.* **2010**, *132*, 4608.
(38) Jansat, S.; Durand, J.; Favier, I.; Malbosc, F.; Pradel, C.; Teuma, E.; Gomez, M. *ChemCatChem.* **2009**, *1*, 224.
(39) Balanta, A.; Godard, C.; Claver, C. *Chem. Soc. Rev.* **2011**, *40*, 4973 , and references therein.
(40) Cote, L. J.; Cruz-Silva, R.; Haung, J. *J. Am. Chem. Soc.* **2009**, *131*, 11027−11032.
(41) Ng, Y. H.; Iwase, A.; Kudo, A.; Amal, R. *J. Phys. Chem. Lett.* **2010**, *1*, 2607−2612.
(42) Li, H.; Pang, S.; Feng, X.; Mullen, K.; Bubeck, C. *Chem. Commun.* **2010**, *46*, 6243−6245.
(43) Vinodgopal, K.; Neppolian, B.; Lightcap, I. V.; Grieser, F.; Ashokkumar, M.; Kamat, P. V. *J. Phys. Chem. Lett.* **2010**, *1*, 1987−1993.
(44) Sokolov, D. A.; Shepperd, K. R.; Orlando, T. M. *J. Phys. Chem. Lett.* **2010**, *1*, 2633−2636.
(45) Abdelsayed, V.; Moussa, S.; Hassan, H. M.; Aluri, H. S.; Collinson, M. M.; El-Shall, M. S. *J. Phys. Chem. Lett.* **2010**, *1*, 2804−2809.
(46) Moussa, S.; Atkinson, G.; El-Shall, M. S.; Shehata, A.; AbouZeid, K. M.; Mohamed, M. B. *J. Mater. Chem.* **2011**, *21*, 9608−9619.
(47) Matsumoto, Y.; Koinuma, M.; Ida, S.; Hayami, S.; Taniguchi, T.; Hatakeyama, K.; Tateishi, H.; Watanabe, Y.; Amano, S. *J. Phys. Chem. C* **2011**, *115*, 19280−19286.
(48) Deryer, D. R.; Park, S.; Bielawski, C. W.; Ruoff, R. S. *Chem. Soc. Rev.* **2010**, *39*, 228−240.
(49) Bagri, A.; Mattevi, C.; Acik, M.; Chabal, Y. J.; Chhowalla, M.; Shenoy, V. B. *Nat. Chem.* **2010**, *2*, 581−587.
(50) Acik, M.; Mattevi, C.; Gong, C.; Lee, G.; Cho, K.; Chhowalla, M.; Chabal, Y. J. *ACS Nano* **2010**, *4*, 5861−5858.
(51) Gómez-Navarro, C.; Meyer, J. C.; Sundaram, R. S.; Chuvilin, A.; Kurasch, S.; Burghard, M.; Kern, K.; Kaiser, U. *Nano Lett.* **2010**, *10*, 1144−1148.
(52) Eda, G.; Fanchini, G.; Chhowalla, M. *Nat. Nanotechnol.* **2008**, *3*, 270−274.
(53) Loh, K. P.; Bao, Q.; Eda, G.; Chhowalla, M. *Nat. Chem.* **2010**, *2*, 1015−1024.
(54) Eda, G.; Lin, Y. Y.; Mattevi, C.; Yamaguchi, H.; Chen, H. A.; Chen, I. S.; Chen., C. W.; Chhowalla, M. *Adv. Mater.* **2010**, *22*, 505−509.
(55) Ito, J.; Nakamura, J.; Natori, A. *J. Appl. Phys.* **2008**, *103*, 113712.
(56) Yan, J.-A.; Xian, L.; Chou, M. Y. *Phys. Rev. Lett.* **2009**, *103*, 086802.
(57) Lahaye, R. J. W. W.; Jeong, H. K.; Park, C. W.; Lee, Y. H. *Phys. Rev. B* **2009**, *79*, 125435.
(58) Hummers, W. S. Jr.; Offeman, R. E. *J. Am. Chem. Soc.* **1958**, *80*, 1339.
(59) Park, S.; Ruoff, R. S. *Nat. Nanotechnol.* **2009**, *4*, 217−224.
(60) Hagland, J.; Fernandez-Guillermat, F.; Grimvall, G.; Korling, M. *Phys. Rev. B* **1993**, *48*, 11685.
(61) Stankovich, S.; Dikin, D. A.; Piner, R. D.; Kohlhaas, K. M.; Kleinhammes, A.; Jia, Y.; Wu, Y.; Nguyen, S. T.; Ruoff, R. S. *Carbon* **2007**, *45*, 1558−1565.
(62) Fan, X.; Peng, W.; Li, Y.; Li, X.; Wang, S.; Zhang, G.; Zhang, F. *Adv. Mater.* **2008**, *20*, 4490.
(63) NIST Database, http://srdata.nist.gov/xps/.
(64) Kudin, K. N.; Ozbas, B.; Schniepp, H. C.; Prud'homme, R. K.; Aksay, I. A.; Car, R. *Nano Lett.* **2008**, *8*, 36−41.
(65) Mkhoyan, K. A.; Contryman, A. W.; Silcox, J.; Stewart, D. A.; Eda, G.; Mattevi, C.; Miller, S.; Chhowalla, M. *Nano Lett.* **2009**, *9*, 1058−1063.
(66) Yeh, T. F.; Syu, J. M.; Cheng, C.; Chang, T. H.; Teng, H. *Adv. Funct. Mater.* **2010**, *20*, 2255−2262.
(67) Tsukahara, Y.; Higashi, A.; Yamauchi, T.; Nakamura, T.; Yasuda, M.; Baba, A.; Wada, Y. *J. Phys. Chem. C* **2010**, *114*, 8965−8970.
(68) Gutmann, B.; Schwan, A. M.; Reichart, B.; Gspan, C.; Hofer, F.; Kappe, C. O. *Angew. Chem., Int. Ed.* **2011**, *50*, 4636−4640.
(69) Horikoshi, S.; Osawa, A.; Serpone, N. *J. Phys. Chem. C.* **2011**, *115*, 23030−23035.
(70) Cassol, C. C.; Umpierre, A. P.; Machado, G.; Wolke, S. I.; Dupont, J. *J. Am. Chem. Soc.* **2005**, *127*, 3298−3299.
(71) Raluy, E.; Favier, I.; Lopez-Vinasco, A. M.; Pradel, C.; Martin, E.; Madec, D.; Teuma, E.; Gomez, M. *Phys. Chem. Chem. Phys.* **2011**, *13*, 13579−13584.
(72) Beletskaya, I. P.; Cheprakov, A. V. *Chem. Rev.* **2000**, *100*, 3009.
(73) Chinchilla, R.; Najera, C. *Chem. Rev.* **2007**, *107*, 874−922.